Neoplasia 47 (2024) 100951

Contents lists available at ScienceDirect

Neoplasia

journal homepage: www.elsevier.com/locate/neo

Original Research

Targeting of oncogenic AAA-ATPase TRIP13 reduces progression of pancreatic ductal adenocarcinoma

Farrukh Afaq [a], Sumit Agarwal [a], Prachi Bajpai [a], Sameer Al Diffalha [a,b], Hyung-Gyoon Kim [a], Shajan Peter [c], Moh'd Khushman [d], Subhash C Chauhan [e], Priyabrata Mukherjee [f], Sooryanarayana Varambally [a,b], Upender Manne [a,b,*]

[a] Department of Pathology, University of Alabama at Birmingham, USA
[b] O'Neal Comprehensive Cancer Center, University of Alabama at Birmingham, USA
[c] Department of Medicine, Division of Gastroenterology, University of Alabama at Birmingham, USA
[d] Department of Medicine, Division of Medical Oncology, Washington University in St. Louis, USA
[e] Department of Immunology and Microbiology, School of Medicine, University of Texas Rio Grande Valley, USA
[f] Department of Pathology, the University of Oklahoma Health Sciences Center, Oklahoma City, Oklahoma, USA

ARTICLE INFO

Keywords:
Pancreatic ductal adenocarcinoma
TRIP13
Tumor progression
Metastasis
Immune response

ABSTRACT

Thyroid hormone receptor-interacting protein 13 (TRIP13) is involved in cancer progression, but its role in pancreatic ductal adenocarcinoma (PDAC) is unknown. Thus, we assessed the expression, functional role, and mechanism of action of TRIP13 in PDAC. We further examined the efficacy of TRIP13 inhibitor, DCZ0415, alone or in combination with gemcitabine on malignant phenotypes, tumor progression, and immune response. We found that TRIP13 was overexpressed in human PDACs relative to corresponding normal pancreatic tissues. TRIP13 knockdown or treatment of PDAC cells with DCZ0415 reduced proliferation and colony formation, and induced G2/M cell cycle arrest and apoptosis. Additionally, TRIP13 knockdown or targeting with DCZ0415 reduced the migration and invasion of PDAC cells by increasing E-cadherin and decreasing N-cadherin and vimentin. Pharmacologic targeting or silencing of TRIP13 also resulted in reduce expression of FGFR4 and STAT3 phosphorylation, and downregulation of the Wnt/β-catenin pathway. In immunocompromised mouse models of PDAC, knockdown of TRIP13 or treatment with DCZ0415 reduced tumor growth and metastasis. In an immunocompetent syngeneic PDAC model, DCZ0415 treatment enhanced the immune response by lowering expression of PD1/PDL1, increasing granzyme B/perforin expression, and facilitating infiltration of CD3/CD4 T-cells. Further, DCZ0415 potentiated the anti-metastatic and anti-tumorigenic activities of gemcitabine by reducing proliferation and angiogenesis and by inducing apoptosis and the immune response. These preclinical findings show that TRIP13 is involved in PDAC progression and targeting of TRIP13 augments the anticancer effect of gemcitabine.

Introduction

Pancreatic ductal adenocarcinoma (PDAC) is an aggressive cancer with a 5-year survival rate of 8 %; worldwide, it is the fourth leading cause of cancer-associated mortality [1]. By 2030, it is projected to become the second leading cause of cancer-related deaths [1,2]. The main causes of high mortality are aggressive tumor biology, anatomical location of the pancreas, advanced stages at the time of diagnosis, and poor response or resistance to conventional chemotherapeutic drugs [3]. Thus, there is a need to identify molecular determinants that regulate the progression of PDAC and serve as therapeutic targets.

Thyroid hormone receptor-interacting protein 13 (TRIP13), an enzyme of AAA-ATPase family, facilitates the assembly or degradation of protein complexes and is involved in various biological functions,

Abbreviations: EMT, epithelial-mesenchymal transition; FGFR4, Fibroblast growth factor receptor 4; LEF1, Lymphoid enhancer factor 1; NSG, NOD/SCID/IL2γ receptor-null; NT, Non-targeting; PD-1, Programmed cell death protein 1; PDAC, Pancreatic ductal adenocarcinoma; PD-L1, Programmed death-ligand 1; STAT3, Signal transducer and activator of transcription 3; TCF1, T-cell factor 1; TME, Tumor microenvironment; TRIP13, Thyroid hormone receptor-interacting protein 13.

* Corresponding author at: Division of Anatomic Pathology, Department of Pathology, Room # 20A, 4th Floor, Wallace Tumor Institute, University of Alabama at Birmingham, Birmingham, AL 35233, USA.
E-mail address: upendermanne@uabmc.edu (U. Manne).

https://doi.org/10.1016/j.neo.2023.100951
Received 15 September 2023; Received in revised form 21 November 2023; Accepted 21 November 2023
Available online 30 November 2023

including spindle assembly checkpoint [4] and DNA repair pathways [5]. Upregulation of TRIP13 contributes to progression of various human cancers, including prostate cancer [6], ovarian cancer [7], hepatocellular carcinoma (HCC) [8], colorectal cancer (CRC) [9–11], breast cancer [12,13], lung adenocarcinoma [14], bladder cancer [15], multiple myeloma [16,17], human papillomavirus-driven cancers [18], and head and neck cancer [19,20]. For glioblastomas, TRIP13 induces its progression through the FBXW7/c-MYC pathway, and its increased expression correlates with poor survival [21]. In B-cell malignances, TRIP13 regulates deubiquitination of tumor suppressor and oncogenic proteins to accelerate tumor progression [22]. In multiple myeloma, aberrant activation of TRIP13 expression promotes EZH2 deubiquitination and thus enhances stemness and drug resistance [23].

Increased expression of TRIP13, regulated by various microRNAs (miR129, miR144, miR-192, miR-515, and miR-4693), PNPT1, and ACTN4, contributes to the pathogenesis of various types of cancers [8,10,11,24–26]. TRIP13 is located at chromosome 5p15.33, and, in lung adenocarcinomas, there is amplification of this region [27]. However, the amplification of *TRIP13* in PDAC is rare (~5 %) (www.cBioPortal.org). A small molecule inhibitor DCZ0415, specifically targeting TRIP13, was developed and tested in multiple myeloma [17] and CRC [28]. However, the oncogenic role of TRIP13 in PDAC progression is not known.

In the present study, we aimed to elucidate the oncogenic role, functional relevance, molecular mechanisms of TRIP13 and evaluate anti-tumor immune response, and clinical significance of inhibiting TRIP13 in PDAC preclinical models. The findings show that TRIP13 acts as an oncogene that promotes PDAC growth and metastasis. Importantly, pharmacological targeting of TRIP13 by DCZ0415 alone and in combination with gemcitabine, a standard first-line treatment for PDAC, effectively inhibits progression of PDACs that overexpress TRIP13.

Materials and methods

Pancreatic tissue specimens

The Anatomic Pathology Division of the University of Alabama at Birmingham (UAB) provided human PDAC samples that were collected from consented PDAC patients after obtaining approval from the UAB Institutional Review Board and Ethics Committee (IRB#060911009). Formalin-fixed, paraffin-embedded (FFPE) PDAC tissue specimens were utilized for immunohistochemical (IHC) studies, and frozen tissues were used for analysis of RNA and protein. The study was conducted in agreement to the standards set by the Declaration of Helsinki.

Cell lines and RNA interference

Human PDAC cell lines (PANC-1, MIA PaCa2 and Bx-PC-3) were procured from ATCC, and S2VP10 cell line was obtained from Prof. Donald J Buchsbaum, University of Alabama at Birmingham. These four human PDAC cell lines (S2VP10, PANC-1, MIA PaCa2, and BxPC-3) exhibiting various mutational statuses of *KRAS, TP53, CDKN2A/p16,* and *SMAD4/DPC4* genes are shown in Supplementary Table 1. PANC-1, MIAPaCa2, BxPC-3, and KPC cells were grown in DMEM media (Corning™ Cellgro™, Fisher Scientific Co., Pittsburgh, PA), and S2VP10 cells were cultured in RPMI media (Corning™ Cellgro™, Fisher Scientific Co., Pittsburgh, PA) containing 1 % penicillin-streptomycin and 10 % fetal bovine serum (FBS, Invitrogen, ThermoFisher Scientific, Carlsbad, CA). The identification and authentication of PDAC cells lines were accomplished at the UAB Heflin Center for Genomic Sciences by performing short tandem repeat DNA profiling. Mycoplasma screening was performed in these cells regularly. Stably inhibiting TRIP13 shRNAs and pGreenPuro^{TM}-expressing lentivectors (Systembio, Palo Alto, CA) generated by the UAB Neuroscience NINDS Vector Core, were used. To infect PDAC cells, lentiviruses expressing TRIP13 shRNA or non-targeting (NT) shRNA were used in the presence of 2 μg/ml polybrene. TRIP13 shRNA sequences are provided in Supplementary Table 2. To generate stable cell lines, puromycin (1 μg/ml) (Life Technologies, ThermoFisher Scientific, Carlsbad, CA) was used as described earlier [10,29,30].

Cell viability assay

The viability of PDAC cells after DCZ0415 treatment was determined by 3-(4,5-dimethylthiazol-2-yl)-2,5-diphenyltetrazolium bromide (MTT) assays. DCZ0415 was obtained from MedChemExpress (Cat. No# HY-130603, Monmouth Junction, NJ) and was dissolved in DMSO. PDAC cells (1×10^3 cells/well) were cultured in 96-well plates and were treated with various concentrations of DCZ0415 (1-30 μM) for 48 or 96 hours. Then 20 μl MTT reagent (5 mg/ml in PBS) obtained from Sigma Aldrich (St. Louis, MO) was added to each well and, after incubation for 2 h, the cells were centrifuged at 1800 g for 10 min. The formazan crystals were dissolved in DMSO, and cell viability was determined at 540 nm using a Synergy™ HTX Multi-Mode Microplate Reader (BioTek, Winooski, VT). The vehicle treated cells were considered as 100 % viable.

Colony formation assay

The formation of colonies was determined as described earlier [10,31,32]. To assess the functional role of TRIP13 on colony formation, TRIP13 knockdown or control NT shRNA-transfected PDAC cells (1×10^3) were cultured in 6-well plates in triplicate. To evaluate the inhibitory effect of DCZ0415 on colony formation, PDAC cells (1×10^3) were cultured in 6-well plates in triplicate overnight. The cells were treated with 10 or 20 μM DCZ0415 and incubated for ten days at 37°C, 5 % CO_2. The cells were then fixed with 5 % glutaraldehyde and stained with crystal violet (Sigma-Aldrich, St. Louis, MO) for 15 minutes. After washing the plates in water, images of colonies were taken with an Amersham Imager 600RGB (GE Healthcare Life Sciences, Pittsburgh, PA).

Cell cycle analysis

PDAC cells (5×10^5 cells/well) were cultured in six-well plates overnight and treated with 10 or 20 μM DCZ0415 for 24 h. The cells were fixed with chilled 70 % ethyl alcohol overnight and were washed twice with PBS, followed by incubation with DNase-free RNase (10 μg/ml) at 37°C for 1 h and then stained with propidium iodide (5 μg/ml) obtained from Sigma Aldrich (St. Louis, MO) for 3 h at 4°C in the dark. Analyses were performed by use of a BD LSR Fortessa™ Flow Cytometer (BD Biosciences, Mountain View, CA).

Western blot analysis

The protein expression in PDAC cells and in tumor lysates was determined by western blotting as described earlier [10,31,32]. Briefly, lysates (30–50 μg protein) were loaded onto NuPAGE™ 4-12 % Bis-Tris Midi Protein Gels (Invitrogen, ThermoFisher Scientific, Carlsbad, CA). The proteins were electro-transferred from the gels onto PVDF membranes (EMD Millipore, Billerica, MA). The membranes were incubated with primary antibodies (see antibody list with their dilutions, catalog numbers, and vendor details in Supplementary Table 3) at 4°C overnight. Further, proteins on the membranes were incubated with HRP-conjugated secondary antibody for 1 h. Signals were developed according to the manufacturer's protocol (EMD Millipore, Billerica, MA).

Invasion assay

The invasive potential of PDAC cells was measured with Transwell BioCoat^{TM} Matrigel matrix (Corning, New York, NY) plates containing

membranes with pores of 8 μm, as described previously [33]. For shRNA studies, TRIP13-silenced PDAC cells (2×10^4) were layered in 24-well plates in serum-free growth medium; for inhibitor studies, DCZ0415 (10 or 20 μM)-treated PDAC cells were plated. To serve as a chemoattractant, the bottom chambers contained growth media with 10 % FBS. After 48 hours of incubation, the invaded cells on the bottom sides of the membranes were fixed in 5 % glutaraldehyde, stained with crystal violet (Sigma Chemical Co., St. Louis, MO), and imaged with a phase-contrast microscope.

Wound healing assay

The migratory potential of PDAC cells was assessed by a wound healing assay, as described earlier [10,31,32]. For shRNA studies, TRIP13-silenced and NT shRNA-transfected PDAC cells (1×10^6), and, for inhibitor studies with DCZ0415, PDAC cells were cultured in 35-mm petri dishes overnight. The next day, artificial wounds were created by using tips of 200-μl pipets, and images were taken and considered as 0 h. The cells were then exposed to DCZ0415 (10 or 20 μM) to determine its effect on migration. At 24 h, photographs were taken from fields of control (NT shRNA-transfected) and TRIP13-silenced cells, and from control and DCZ0415-treated PDAC cells.

Toxicity assessments

Toxicity assessments of DCZ0415 were performed with immunocompromised NOD/SCID/IL2γ receptor null (NSG) and immunocompetent (C57BL/6J) mice obtained from the Jackson Laboratory (Farmington, CT). At UAB, the mice were housed in an animal facility under pathogen-free conditions. All animal experiments were approved by the UAB Institutional Animal Care and Use Committee (IACUC-21501). NSG and C57BL/6J mice (n = 3, in each group) were dosed with vehicle or DCZ0415 (25 mg/kg). DCZ0415, dissolved in DMSO (10 %)+ PEG300 (40 %)+ Tween-80 (5 %) and saline (45 %), was administered intraperitoneally (i.p.) on alternate days. At weeks 1, 2, and 4, blood was collected from these mice, and serum was isolated. The quantitative determination of urea nitrogen (BUN), alkaline phosphate (ALP), alanine aminotransferase (ALT), inorganic phosphorus, total protein, calcium, and total bilirubin was accomplished with a SIRRUS Stanbio (Stanbio Laboratory, Boerne, TX) automated chemical analyzer. Similarly, we also assessed, at week 2, the toxicity of the vehicle, DCZ0415 (10 mg/kg; every alternate/day), gemcitabine (10 mg/kg, twice/week), and their combination (DCZ0415+ gemcitabine) with C57BL/6J mice. Gemcitabine was obtained from Selleck Chemicals LLC (Catalog # LY-18801, Houston, TX) and dissolved in DMSO (10 %)+ PEG300 (40 %)+ Tween-80 (5 %) and saline (45 %).

Subcutaneous and orthotopic mouse models

Subcutaneous and orthotopic injections were performed with NSG (6–8 weeks old) mice. To determine the functional role of TRIP13 on PDAC tumor growth, S2VP10 cells (1×10^6) transfected with NT shRNA or TRIP13 shRNA were injected subcutaneously into NSG mice. For DCZ0415 inhibitor studies, S2VP10 cells were injected subcutaneously into mice and, when the tumor volume reached approximately 100 mm^3, mice were randomly assigned to a vehicle group (n = 6) or to a group for dosing with DCZ0415 (25 mg/kg) administered i.p. every other day. Tumor volumes were measured regularly and calculated with the formula, 0.5 × tumor length × tumor $width^2$. Mice were monitored for general health symptoms and were euthanized when they reached the experimental endpoint. At termination of the experiments, tumors were harvested for hematoxylin and eosin (H&E), IHC, and western blot analyses.

For developing orthotopic PDAC models, S2VP10-Luc cells (1×10^6) were injected orthotopically into the pancreas of NSG mice. The mice were randomly divided into two groups and treated with vehicle or DCZ0415 (25 mg/kg every alternate day) until termination of the experiments. To measure tumor growth non-invasively by luciferase activity, the mice were injected i.p. with D-luciferin (100 μl/mouse of 10 mg/ml in PBS) at different time intervals; tumor growth was determined by use of an *In Vivo* IVIS Lumina Series III spectrum imaging system (Perkin Elmer, Waltham, MA).

Experimental metastasis mouse model

To evaluate the effects of TRIP13 knockdown or treatment with DCZ0415 on experimental metastases, we utilized NSG mice. For TRIP13 knockdown studies, S2VP10-Luc cells (1×10^6) transfected with NT shRNA or TRIP13 shRNA were injected into the tail veins of NSG mice (6–8 weeks), as described previously [10,28]. For DCZ0415 studies, S2VP10-Luc cells (1×10^6) were injected into the tail veins of NSG mice. After injection of cells, the mice were randomly divided into two groups and treated with vehicle or DCZ0415 (25 mg/kg every alternate day) until termination of the experiments. For combination studies, S2VP10-Luc cells were injected into the lateral tail veins of NSG mice, which were randomly divided into four groups with five animals in each group. The first group of mice received vehicle and served as controls. The second group received DCZ0415 (25 mg/kg/every alternate day). The third group received gemcitabine (10 mg/kg/twice per week), and the fourth group received both DCZ0415 (25 mg/kg; every alternate day) and gemcitabine (10 mg/kg mg/kg/twice per week). The mice were dosed i.p. with these agents and were imaged every week for metastasis by bioluminescent imaging as described above. The mice were euthanized at the end of the experiments, and their organs were harvested for assessment of metastases by H&E staining.

Immunocompetent syngeneic KPC mouse model

To examine the effects of test agents (DCZ0415, gemcitabine, and their combination), murine KPC cells (0.1×10^6) were subcutaneously injected into male and female C57BL/6J mice (6-8 weeks). In the first study, when the tumor volume reached approximately 200 mm^3, animals were randomly divided into vehicle ($n = 5$) and DCZ0415 ($n = 5$) treatment groups. DCZ0415 (25 mg/kg) was injected i.p. every alternate day. In the second study, when tumors reached approximately 200 mm^3, animals were randomly divided into vehicle ($n = 5$), DCZ0415 ($n = 5$), gemcitabine (n=5), and DCZ0415+ gemcitabine (n=5) treatment groups. DCZ0415 (25 mg/kg, i.p.) was injected every alternate day and gemcitabine (25 mg/kg, i.p.) twice per week. Combination index (CI) values (additive/synergistic) for DCZ0415 and gemcitabine were calculated by Bliss-independent equations as described earlier [34]. These studies were performed in agreement with the approved IACUC-21501 protocol. At termination of the experiment, tumors were collected for H&E, IHC, and western blotting.

Immunohistochemical (IHC) analysis

From mice, tumors were harvested and fixed in formalin and embedded in paraffin. Sections were cut for IHC analysis accomplished as described earlier [28]. In brief, sections were deparaffinized in xylene and rehydrated in ethanol. Antigen retrieval was performed at 100°C for 30 minutes in citrate buffer (pH 6.0) followed by incubation with primary and secondary antibodies. The details of the antibodies and their dilutions are summarized in Supplementary Table 3. The slides were developed in diaminobenzidine (Cat# SK-4100, Vector Laboratories) and counter-stained with hematoxylin QS (Cat#H-3404; Vector Laboratories). The stained slides were mounted with VectaMount Permanent Mounting Medium (Cat#H-5000; Vector Laboratories), and images were captured.

Statistical analysis

A Student's *t*-test was employed, and *P*-values < 0.05 were considered statistically significant. The data were expressed as means ± standard deviation.

Results

High expression of TRIP13 in PDACs

By use of UALCAN (https://ualcan.path.uab.edu) [35,36], a web resource for analyzing cancer transcriptomic/proteomic data, we compared TRIP13 mRNA and protein expression between PDACs and corresponding normal pancreatic tissues available from TCGA and CPTAC [37] found that, in PDACs, the TRIP13 mRNA/protein levels were upregulated (Fig. 1A, B). We validated the observations from the TCGA pancreatic cancer transcriptomic sequencing and CTPAC proteomics data by performing qPCR and western blotting in normal and PDAC tissues; the data showed overexpression of TRIP13 at mRNA and protein levels in tumors as compared to normal pancreases (Fig. 1C, D). We further performed IHC staining using TRIP13-specific antibodies to evaluate the protein expression patterns of the TRIP13 in PDAC tissues.

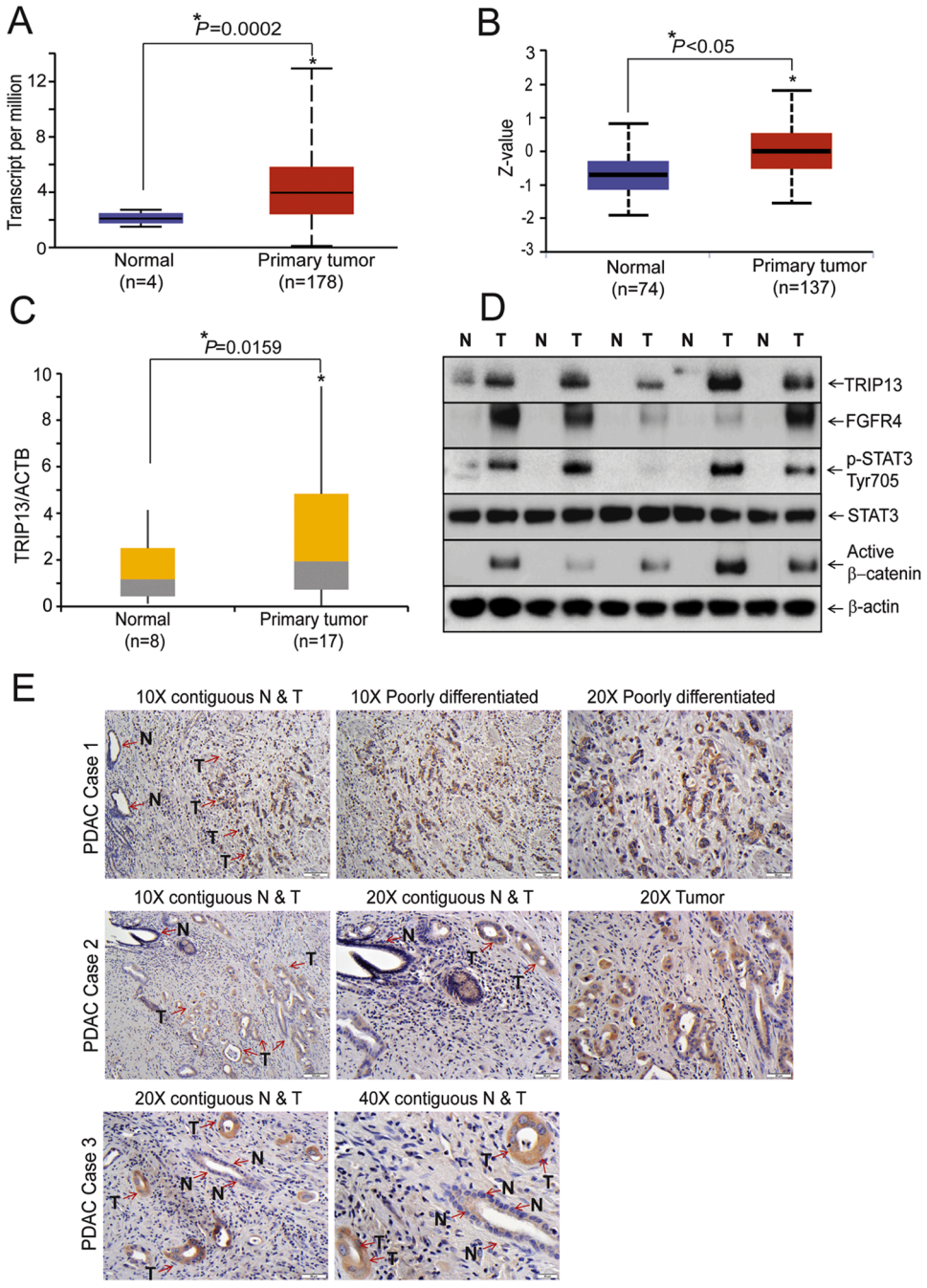

Fig 1. TRIP13 overexpression in PDACs. (A-B) Analyses of UALCAN data from TCGA and CPTAC for TRIP13 mRNA and protein expression in normal pancreas and primary PDAC samples. The numbers of subjects in each group are indicated in parentheses. (C) qPCR data analysis showing the expression of TRIP13 in PDACs compared to normal pancreas. (D) Western blot analysis for TRIP13, FRGF4, pSTAT3, STAT3, and active β-catenin in normal pancreas (N) and PDAC (T) samples. These N and T corresponding samples were procured from patient with PDAC. Samples of 5 PDAC patients were analyzed by western blot analysis. (E) IHC analysis at various magnifications showing the staining of TRIP13 in 3 cases of PDAC tissues having adjacent normal tissue. Scale bar of 10x-100 μm; 20x-50 μm, and 40x-20 μm.

IHC staining showed high expression of TRIP13 in PDACs relative to normal pancreatic tissues; the staining was present primarily in the cytoplasm (Fig. 1E). Notably, TRIP13 protein expression was higher in PDAC samples with receptor tyrosine kinase (RTK) alterations (Supplementary Fig. 1). TRIP13 overexpression in PDAC samples activated FGFR4, an RTK. Further, PDAC samples with high TRIP13 expression showed elevated phosphorylation of STAT3 at Tyr705, and high levels of active β-catenin (Fig. 1D). These findings that high expression of TRIP13, at the mRNA and protein levels, in human PDACs led to investigations of how upregulated TRIP13 mediates PDAC progression.

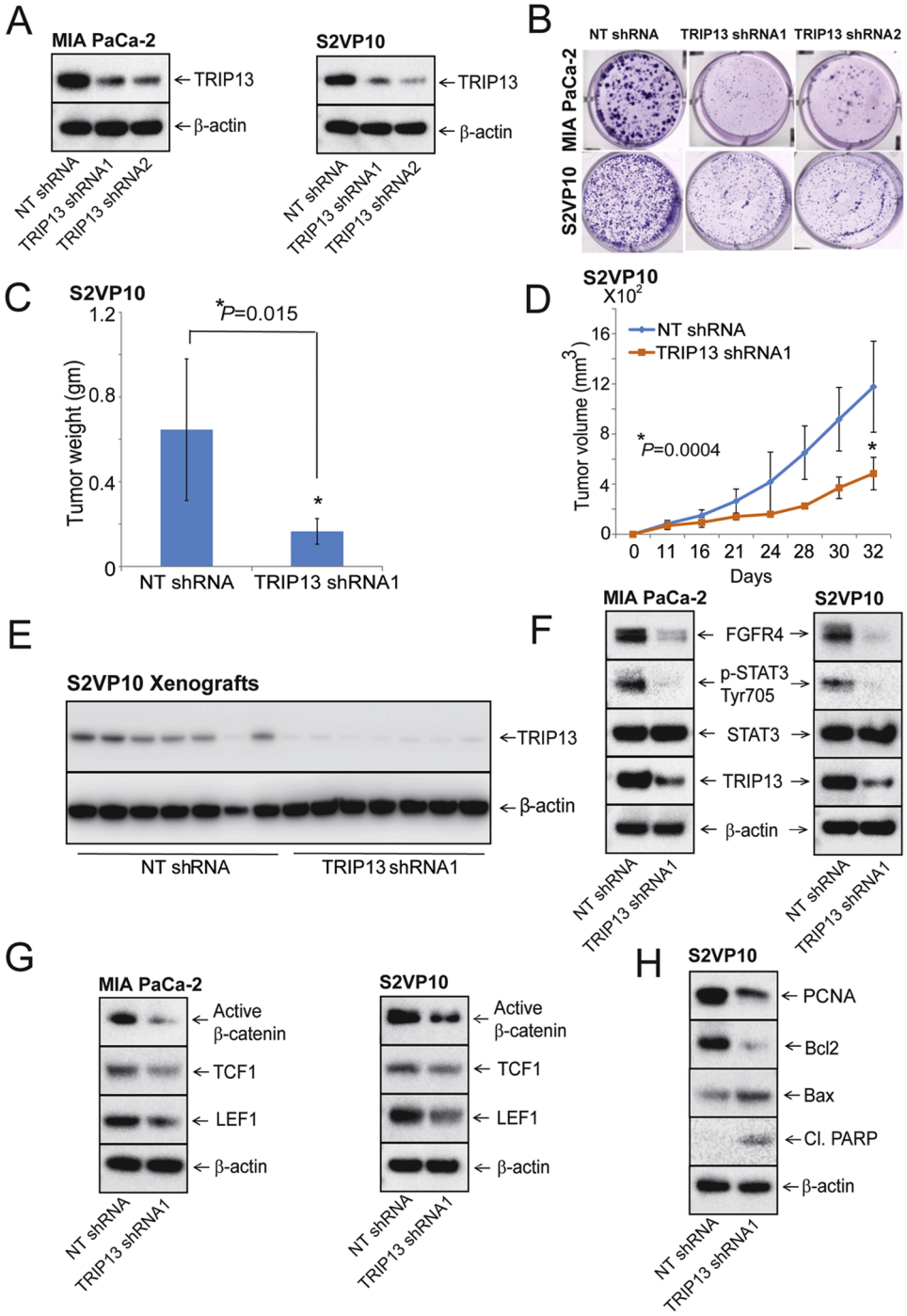

Fig 2. TRIP13 induces aberrant activation of FGFR4/STAT3/β-catenin, leading to increased colony formation and PDAC progression. (A) Western blotting showing the expression of TRIP13 in PDAC cell lysates of TRIP13 knockdown and NT shRNA cells; *β*-actin was used to assure equal loading of protein. (B) TRIP13 knockdown in PDAC cells reduced colony formation. (C) Weights were measured in TRIP13 shRNA and TRIP13 NT shRNA tumors. Error bars indicate means ± SD, $^*P = 0.015$. (D) Statistical analysis of the volumes (mm^3) versus time in TRIP13 shRNA and TRIP13 NT shRNA tumors. Error bars indicate means ± SD, $^*P = 0.0004$. (E) Lysates from PDAC xenografts with TRIP13 shRNA or NT shRNA were subjected to western blotting and probed for TRIP13. (F) Expression of FGFR4, pSTAT3, STAT3, and TRIP13 in PDAC cell lysates after TRIP13 knockdown. (G) Expression of active β-catenin, TCF1, and LEF1. (H) Expression of PCNA, Bcl2, Bax, and cleaved PARP. Equal loading was confirmed by probing the membrane for β-actin.

TRIP13 knockdown suppresses PDAC progression by downregulating the expression of FGFR4, pSTAT3, and β-catenin

We first examined the protein levels of TRIP13 in four PDAC cell lines (BxPC-3, MIA PaCa-2, S2VP10, and PANC-1) with various genetic backgrounds (Supplementary Table 1). Western blotting showed that all four PDAC cell lines expressed high levels of TRIP13 protein (Supplementary Fig. 2A). To investigate its functional role, we silenced TRIP13 in PDAC cells with a lentivirus transfection using specific shRNA targeting TRIP13 [10]. Stable inhibition of TRIP13 was confirmed by western blotting showing reduced TRIP13 protein (Fig. 2A). Moreover, data from clonogenic assays revealed that TRIP13 knockdown diminished colony formation compared to control shRNA (Fig. 2B). In addition, we determined the role of TRIP13 on tumor growth by using an S2VP10 xenograft model. Tumors formed with S2VP10 cells exhibiting TRIP13 shRNA had lower weights (Fig. 2C) and grew slower than those with TRIP13 NT shRNA (Fig. 2D). These data indicated that TRIP13 knockdown contributed to alleviating PDAC progression. Western blot

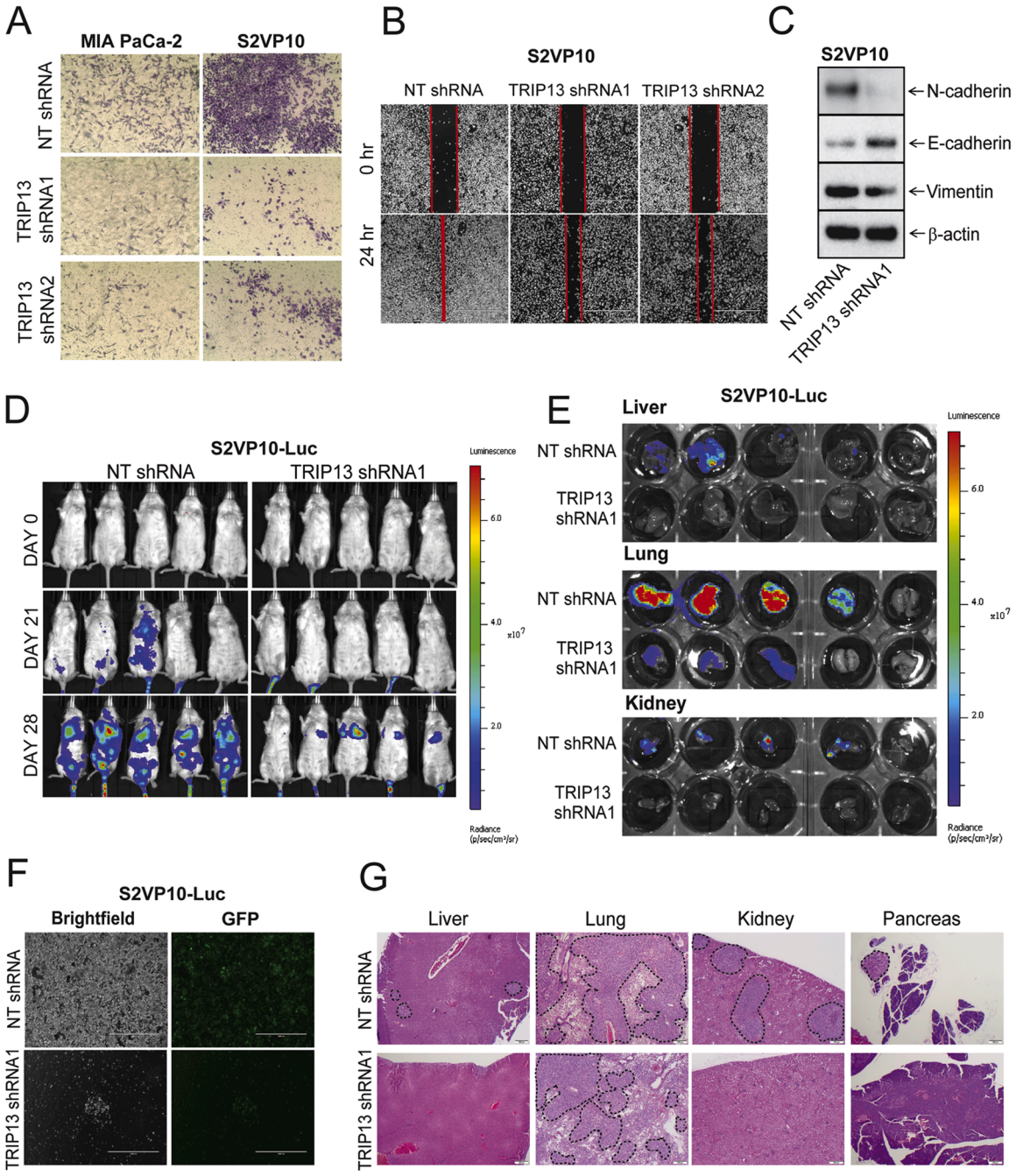

Fig 3. TRIP13 silencing decreases migration, invasion, and metastasis of PDAC cells. (A) Invasion assay performed with TRIP13-silenced PDAC cells. (B) Wound-healing assays were used to examine the migration of PDAC cells after TRIP13 knockdown. Wound closure was determined after 24 h. (C) EMT protein expression in TRIP13-knockdown PDAC cells. (D) PDAC cells stably expressing luciferase reporter (S2VP10-Luc, 1.0×10^6 cells) were injected into tail veins of NSG mice. Mice were imaged every week with an IVIS imaging system to monitor metastasis. (E) *Ex vivo* luminescence of liver, lung, and kidney. (F) Bone marrow of mice was flushed and cultured in media. Representative phase contrast and GFP images taken at day 21 showing bone marrow or cancer cells obtained from bone marrow of mice injected with S2VP10 cells exhibiting NT shRNA or TRIP13 shRNA. Scale bar: 1000 μm. (G) H&E staining of lung, liver, kidney, and pancreas from S2VP10 cells transfected with TRIP13 shRNA or NT shRNA. Dotted lines show metastatic lesions. Scale bar: 200 μm.

analyses of xenograft tumors were performed to validate the knockdown efficiency of TRIP13 (Fig. 2E). These results reveal that TRIP13 knockdown attenuates colony formation and tumor growth.

Since FGFR4, STAT3, and Wnt/β-catenin signaling pathways are implicated in PDAC progression and drug resistance [38,39], we investigated the role of TRIP13 in regulating these signaling molecules. Cells with TRIP13 knockdown showed decreased expression of FGFR4 and reduced STAT3 phosphorylation at Tyr705 (Fig. 2F). In these cells,

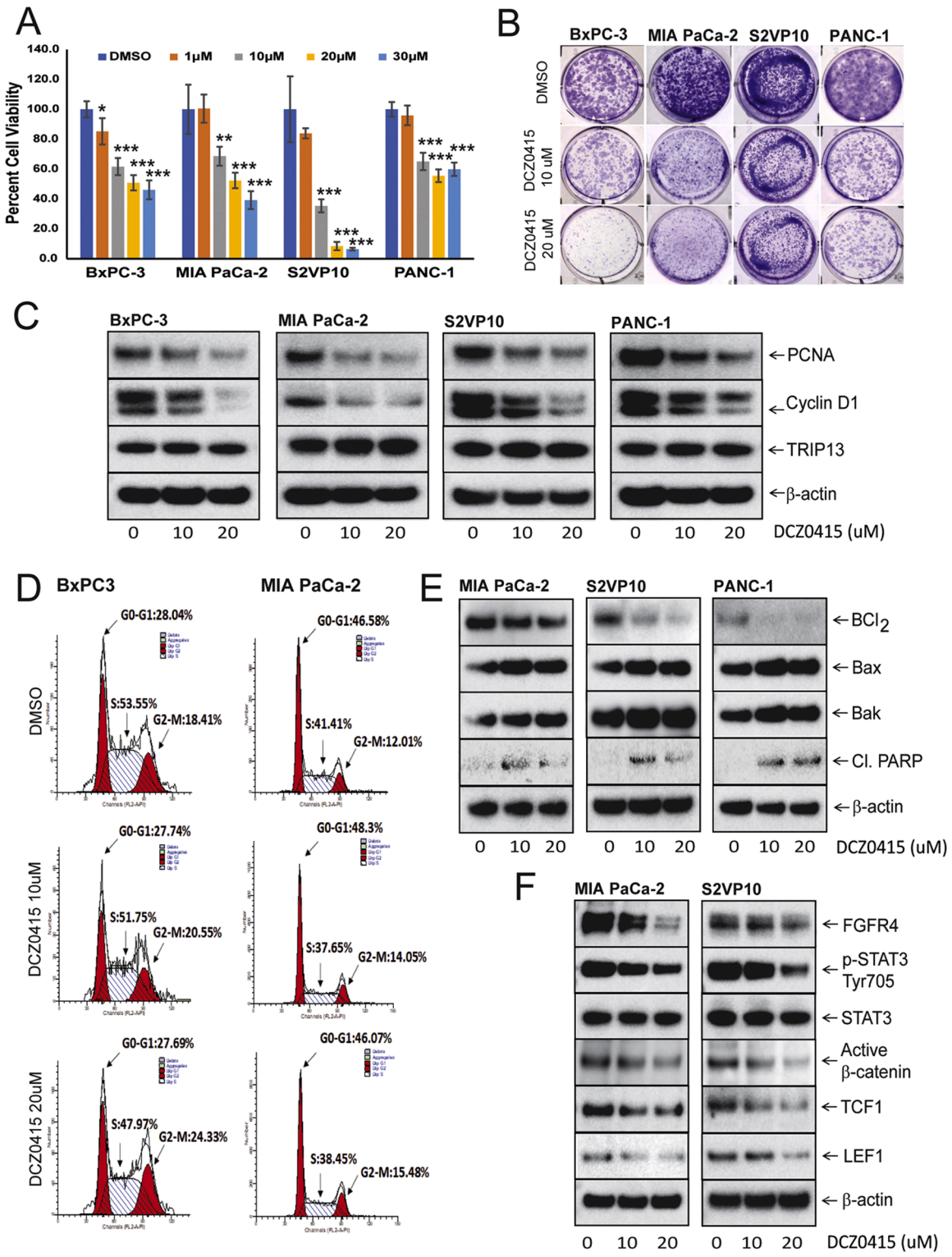

Fig 4. DCZ0415 treatment reduces aggressive phenotypes by downregulating FGFR4/STAT3/β-catenin in PDAC cells. (A) Cell viability was evaluated by MTT assays after treatment of PDAC cells with DCZ0415 (1-30 μM) for 96 h. Error bars indicate means ± SD, *P < 0.05; **P < 0.01; ***P < 0.001 versus control. (B) Colony assay performed after vehicle and DCZ0415 (10 or 20 μM) treatment; the colonies were stained with crystal violet. (C) Western blot analysis showing expression of PCNA, cyclin D1, and TRIP13 in DCZ0415-treated PDAC cells. (D) The cell cycle was assessed by flow cytometry. (E) Expression of Bcl2, Bax, Bak, and cleaved PARP. (F) Expression of FGFR4, pSTAT3, STAT3, and β-catenin signaling molecules. Equal loading was confirmed by probing the membrane for *β*-actin.

TRIP13 knockdown lowered the expression of active-β-catenin, LEF1, and TCF1 as compared to cells with control shRNA (Fig. 2G). Furthermore, silencing of TRIP13 reduced expression of proliferating cell nuclear antigen (PCNA) and induced poly-ADP ribose polymerase (PARP) cleavage by modulating Bcl2 family proteins (Fig. 2H). These data establish a link between TRIP13 and the FGFR4/STAT3 and Wnt/β-catenin signaling molecules a mechanism that contribute to PDAC progression.

TRIP13 knockdown reduces PDAC migration, invasion, and metastasis by modulating the epithelial-mesenchymal transition (EMT)

We investigated the role of TRIP13 silencing on invasion and migration of PDAC cells and observed that the invasive and migratory potentials of PDAC cells were reduced by TRIP13 silencing compared to controls (Fig. 3A, B). Since the EMT is implicated in tumor cell invasion and migration, we analyzed the expression of EMT markers to determine the role of TRIP13. TRIP13 knockdown elevated expression of the epithelial marker, E-cadherin, but reduced expression of the mesenchymal markers, N-cadherin and vimentin (Fig. 3C), indicating that TRIP13 promotes EMT in PDAC.

Next, we assessed whether TRIP13-knockdown reduces metastasis in an experimental NSG mice model. We injected S2VP10-Luc cells intravenously and followed the kinetics of metastasis by quantitative bioluminescence imaging (BLI). Downregulation of TRIP13 delayed the onset of metastasis to distant organs as established by BLI (Fig. 3D). Moreover, *ex vivo* BLI imaging showed low luminescence activity in liver, lung, kidney, bone and pancreases in the TRIP13-knockdown group of mice as compared to the NT shRNA control group (Fig. 3E; Supplementary Fig. 3A). In *ex vivo* experiments, mouse bone marrow cultures, consisting of PDAC cells (ST2VP10-Luc) with NT shRNA or TRIP13 shRNA were tracked to assess the extent of metastasis. In TRIP13 knockdown cells, the numbers of PDAC cells were reduced in bone marrow cultures at 7 and 14 days (Supplementary Fig. 3B), and 21 days (Fig. 3F) as compared to NT shRNA controls. Consistently, H&E staining showed less metastatic nodules in the liver, lung, kidney, and pancreas of mice with TRIP13 shRNA compared to control NT shRNA tumors (Fig. 3G). Overall, the data obtained from *in vitro* and *in vivo* models indicate that TRIP13 plays a role in migration, invasion, and metastasis of PDAC by modulating EMT markers.

TRIP13 inhibitor DCZ0415 reduces cell growth and colony formation by modulating Bcl2 family proteins and downregulating FGFR4/STAT3// β-catenin signaling

Next, we assessed the inhibitory effects of DCZ0415, a TRIP13 targeting small molecule inhibitor, on the growth of PDAC cells by using MTT assays. DCZ0415 treatment reduced PDAC cell growth in a dose- and time-dependent fashion (Fig. 4A, Supplementary Fig. 2B). Furthermore, DCZ0415 reduced the numbers of colonies formed by PDAC cells (Fig. 4B). Treatment of PDAC cells with DCZ0415 also caused inhibition of PCNA and cyclin D1 (Fig. 4C), established markers of cell proliferation. We next determined whether its effects were due to cell cycle arrest. Flow cytometry data indicated that treatment of PDAC cells (BxPC3 and MIA PaCa-2) with DCZ0415 resulted in increased cell populations in the G_2/M phase and reduction in the S phase of the cell cycle (Fig. 4D). Furthermore, we determined the effect of DCZ0415 on Bcl2 family proteins, which can be either pro-apoptotic or anti-apoptotic. DCZ0415 treatment decreased the expression of Bcl2 (anti-apoptotic) and increased the expression of Bax and Bak (pro-apoptotic) proteins (Fig. 4E). In addition, DCZ0415, by modulating Bcl2 family proteins, induced apoptosis, as shown by elevated PARP cleavage (Fig. 4E). Then, we examined the mechanism(s) of action of DCZ0415 in PDAC cells. DCZ0415 reduced the expression of FGFR4 and phosphorylation of STAT3 at Tyr705. Furthermore, there was reduced expression of active β-catenin, LEF1, and TCF1 (Fig. 4F). These findings indicate that, in PDAC cells, DCZ0415 inactivates the TRIP13/FGFR4/STAT3 axis and the Wnt/β-catenin signaling pathway, leading to reduced cell proliferation and induction of apoptosis by modulating Bcl-2 proteins.

Toxicity assessment of DCZ0415 and its effect on progression of PDAC in immunocompromised subcutaneous and orthotopic mouse models

We performed a toxicity assessment with immunocompromised NSG mice treated with vehicle or DCZ0415. When serum samples were analyzed at weeks 1, 2, and 4, DCZ0415-treated mice did not show any sign of toxicity (Supplementary Table 4). The toxicity parameters analyzed in serum of mice treated with vehicle or DCZ0415 were similar, and the values were in the reference range, as published earlier [40,41]. Next, we determined the effect of DCZ0415 on tumor growth in subcutaneous and orthotopic NSG models. Subcutaneous injections of S2VP10 cells treated with DCZ0415, resulted in reduction of tumor weight (Fig. 5A) and tumor volume (Fig. 5B) compared to control mice. Additionally, histomorphology evaluation of H&E-stained sections showed no signs of toxicity in livers and kidneys obtained from these mice after administration of vehicle or DCZ0415 (Fig. 5C). Xenograft tumor tissues of DCZ0415-treated mice showed lower expression of FGFR4 and p-STAT3 at Tyr705 residue compared to tumor tissues of vehicle-treated mice (Fig. 5D). Furthermore, we examined if, in mice, DCZ0415 exerted its anti-tumor effect through regulating the Wnt/β-catenin signaling pathway. In tumors collected from DCZ0415-treated mice, there were lower expressions of active β-catenin, LEF1, TCF1, and cyclin D1 as compared to tumors collected from vehicle-treated mice (Fig. 5E), indicating an inhibitory effect of DCZ0415 on PDAC growth by downregulation of the Wnt/β-catenin pathway. These *in vivo* data were consistent with the *in vitro* findings. Furthermore, tumors of DCZ0415-treated mice had high expression of E-cadherin, an epithelial marker, and low expressions of N-cadherin and vimentin, which are mesenchymal markers (Fig. 5F), indicating that, by reversing the EMT process, DCZ0415 inhibits progression of PDAC in mice.

To assess the antitumor effect of DCZ0415, we used an established, a disease-relevant orthotopic model with luciferase-expressing S2VP10 cells. Treatment with DCZ0415 repressed the growth of tumors in the pancreas of mice (Fig. 5G). These data show that DCZ0415 acts as an anti-tumorigenic agent by downregulating the FGFR4/pSTAT3/Wnt/β-catenin signaling pathway.

DCZ0415 reduces invasion, migration, and metastasis of PDAC cells

The PDAC cells that were treated with DMSO migrated rapidly toward closing the gap produced by a scratch; however, DCZ0415-treated cells showed less movement, demonstrating that it decreased their migratory potential (Fig 6A). Moreover, Transwell invasion assays revealed lower numbers of invasive cells compared to the control group (Fig. 6B). Treatment of PDAC cells with DCZ0415 decreased N-cadherin and vimentin expression and increased E-cadherin expression (Fig 6C). For MIA PaCa-2 cells, there was no expression of E-cadherin protein, as these cells do not express it [42]. Thus, DCZ0415 decreases migration and invasion of these cells by modulating EMT proteins.

To assess whether DCZ0415 has anti-metastatic efficacy in mice, we performed a study with NSG mice injected intravenously with S2VP10-Luc cells. DCZ0415 treatment reduced metastasis to distant organs compared to vehicle-treated mice (Fig. 6D). This was confirmed by H&E staining, which showed small metastatic nodules in the lung, liver, kidney, and pancreas of DCZ0415-treated mice compared to vehicle-treated mice (Fig. 6E). These data reveal that, by modulating EMT markers, targeting of TRIP13 with DCZ015 inhibits cell migration, invasion, and metastasis.

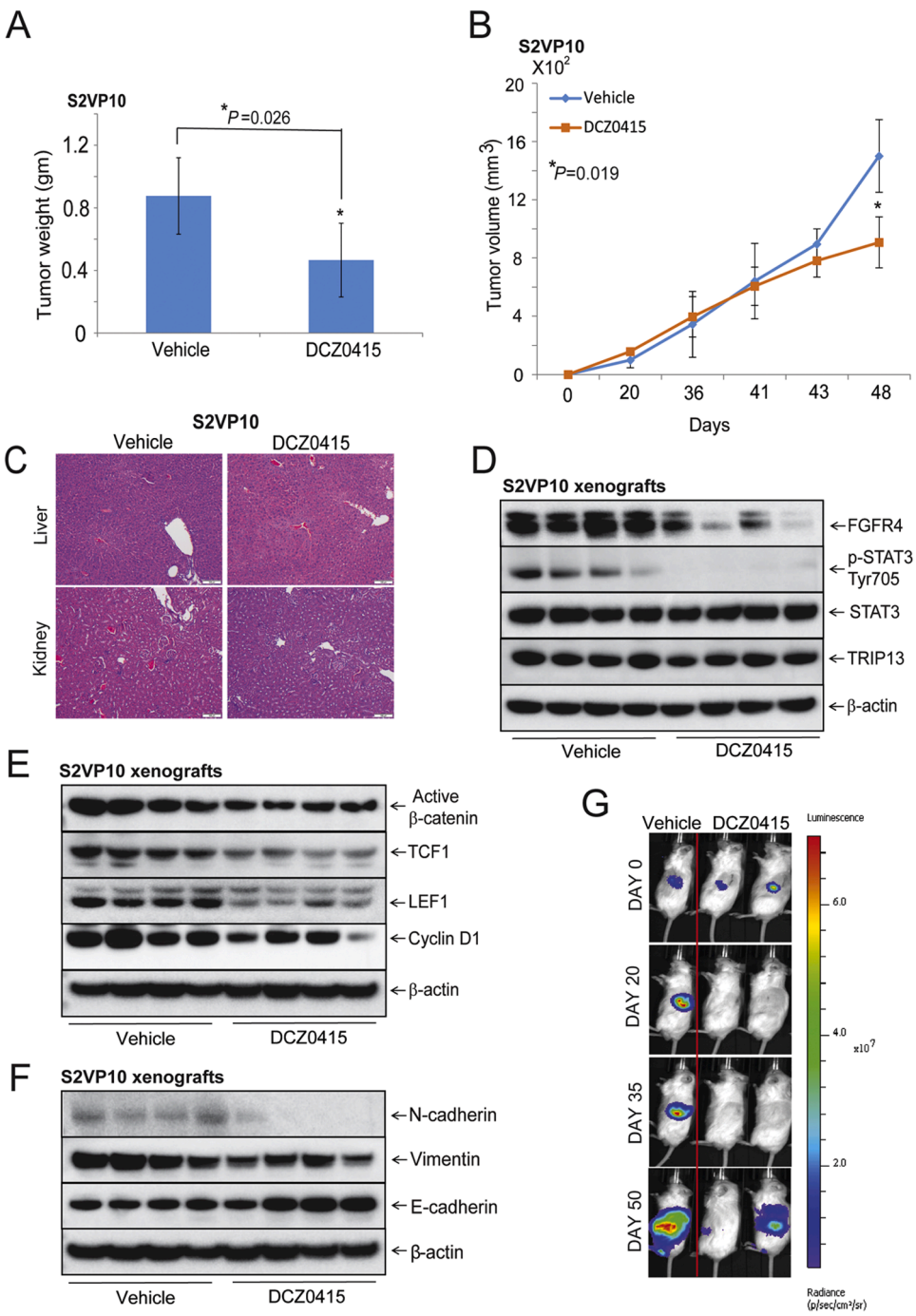

Fig 5. DCZ0415 treatment decreases tumor growth in PDAC xenografts and orthotopic mouse models, and downregulates FGFR4, pSTAT3 and β-catenin signaling. NSG mice were treated with 25 mg/kg of DCZ0415 or vehicle control every alternate day until termination of the experiments (A) Quantitative analysis of tumor weights for vehicle- and DCZ0415-treated groups. Error bars indicate means ± SD, $^*P = 0.026$. (B) Tumor volumes are shown for vehicle- and DCZ0415-treated animals. Error bars indicate means ± SD, $^*P = 0.019$. (C) H&E staining of liver and kidney of mice treated with vehicle or DCZ0415. (D) Expressions of FGFR4, pSTAT3, STAT3, and TRIP13. (E-F) Expression of β-catenin signaling molecules and EMT proteins in vehicle- and DCZ0415-treated tumors. Equal loading was confirmed by probing the membrane for β-actin. (G) Luciferase expressing S2VP10 cells (1.0×10^6) were injected orthotopically into the pancreases of NSG mice, and mice were treated with vehicle or 25 mg/kg DCZ0415 every alternate day until termination of the experiments.

DCZ0415 reduces PDAC progression and enhances anti-tumor immunity in an immunocompetent syngeneic mouse model

To investigate the effect of targeting TRIP13 with DCZ0415 on tumor growth and immune response, we utilized immunocompetent PDAC (KPC)- syngeneic (C57BL/6J) mouse model. Compared with the vehicle control, DCZ0415 treatment significantly reduced tumor weight (Fig. 7A) and tumor volume (Fig. 7B). IHC staining revealed that DCZ0415-treated tumors showed low expression of PCNA, a proliferative marker, and high expression of active caspase 3, an apoptotic marker (Fig 7C). The data indicate that the reduction in tumor growth by DCZ0415 was due to a decrease in cell proliferation and an increase in apoptosis. Furthermore, analyses of serum samples collected from DCZ0415-treated mice did not show any sign of toxicity at weeks 1, 2, and 4 (Supplementary Table 5).

Next, we determined whether DCZ0415 treatment increased anti-

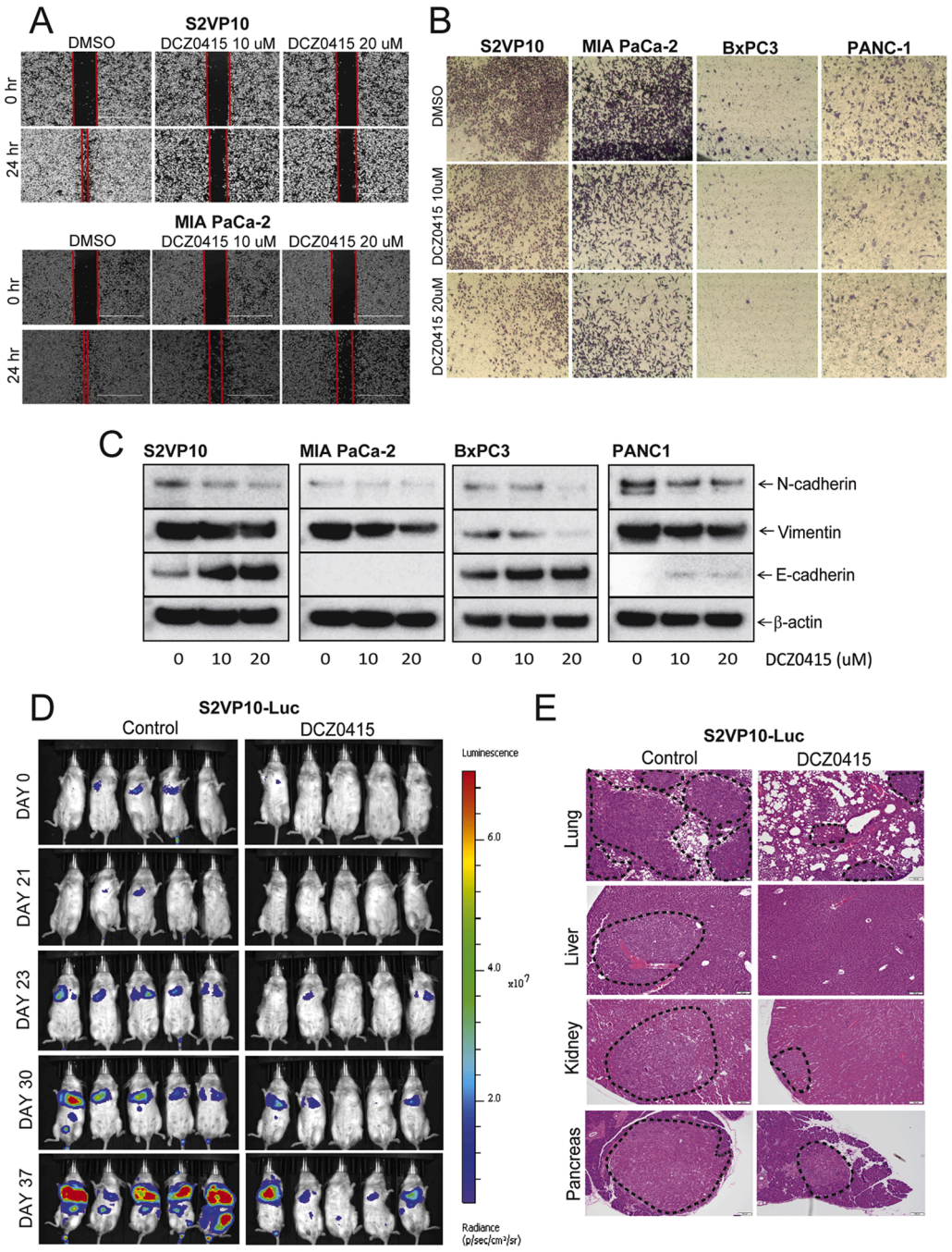

Fig. 6. DCZ0415 treatment decreases migration, invasion, and metastasis of PDAC cells. (A) A wound-healing assay was performed to determine the migratory capacity of PDAC cells treated with vehicle or DCZ0415. Wound closure was determined after 24 hours. (B) An invasion assay was performed with vehicle- and DCZ0415-treated PDAC cells. (C) Expression of EMT proteins was determined in PDAC cells after DCZ0415 treatment. (D) S2VP10-Luc cells (1.0×10^6) were injected into tail veins of NSG mice. Metastasis was monitored every week with an IVIS imaging system. (E) H&E showing metastasis of S2VP10 cells to lung, liver, kidney, and pancreas. Dotted lines show metastatic lesions. Scale bar: 200 μm.

tumor immunity in syngeneic mouse tumors. Western blot analysis revealed that DCZ0415 induced an immune response by increasing the expression of cytotoxic mediator markers, granzyme B and perforin (Fig. 7D). In addition, DCZ0415 treatment increased its cytotoxic effect by decreasing the expression of immune checkpoint molecules, programmed cell death-1 (PD-1) and programmed cell death-ligand 1 (PD-L1) (Fig. 7D,E). Furthermore, DCZ0415 treatment increased infiltration of CD3 and CD4 T cells (Fig. 7E). These data indicate that, in a PDAC syngeneic mouse model, the TRIP13 inhibitor reduced tumor growth by decreasing proliferation, inducing apoptosis, and activating anti-tumor immunity.

DCZ0415 in combination with gemcitabine enhances therapeutic efficacy in immunocompromised and immunocompetent PDAC mouse models

We examined the effects of DCZ0415; gemcitabine, a synthetic pyrimidine nucleoside analogue used as a standard first-line treatment for PDAC; and their combination on tumor growth in immunocompetent C57BL/6J mice by subcutaneously implanting KPC cells. The combination treatment was highly effective in reducing tumor size, weight, and growth kinetics as compared with DCZ0415 or gemcitabine alone (Fig. 8A-C). The Bliss-independent equation was used to calculate combination index (CI) values for DCZ0415, gemcitabine, and their

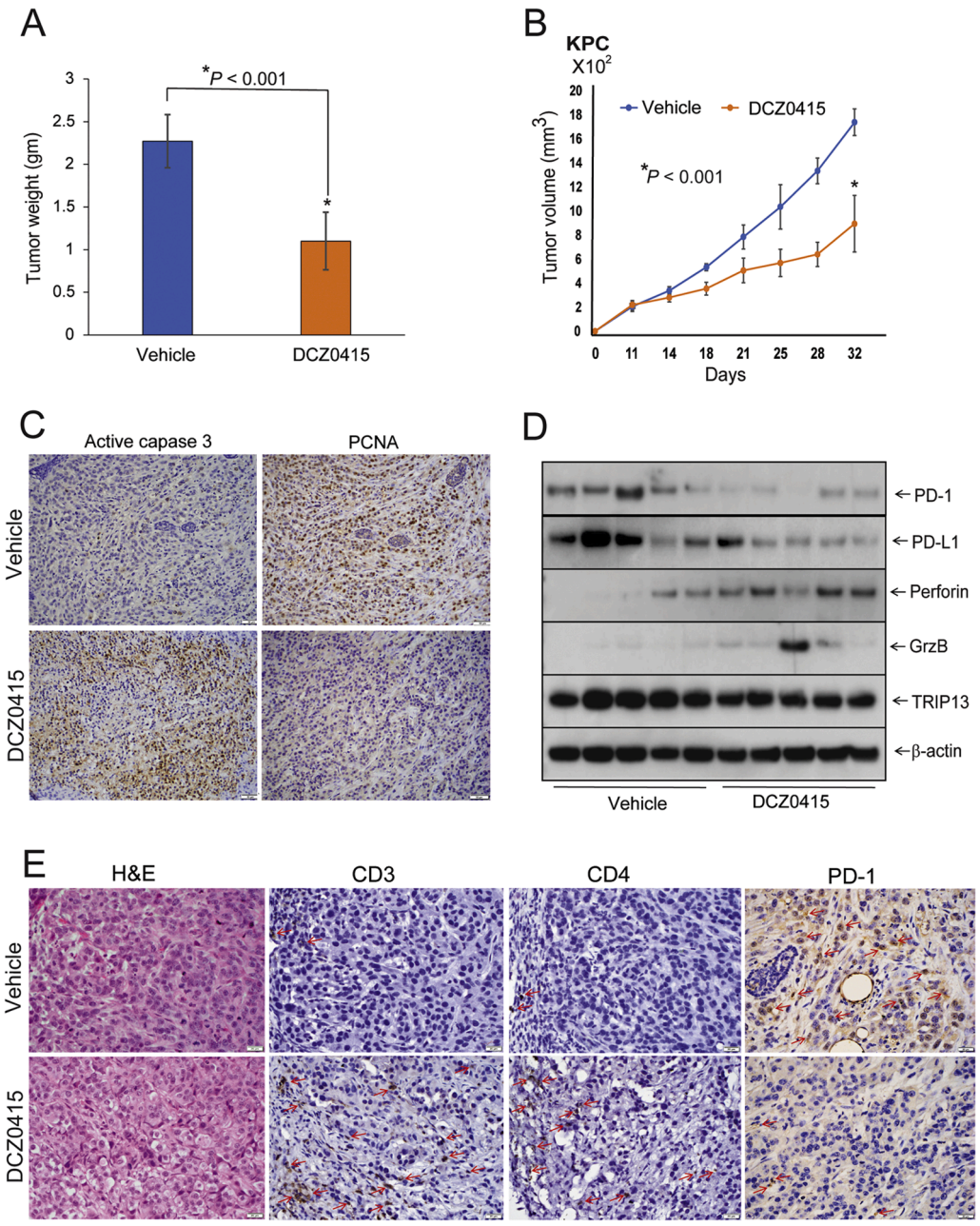

Fig. 7. DCZ0415 treatment reduces tumor growth and increases immune response in an immunocompetent syngeneic PDAC model. (A) Tumor weights of mice treated with vehicle or DCZ0415. These tumors were generated in C57BL/6J mice by implanting KPC cells (0.1×10^6). Error bars indicate means ± SD, $^*P < 0.001$. (B) Tumor volume of mice treated with vehicle or DCZ0415. Error bars indicate means ± SD, $^*P < 0.001$. (C) IHC staining showing protein expression of active-caspase 3 and PCNA in mice tumors treated vehicle or DCZ0415. Scale bar: 50 μm. (D) Western blotting showing protein expression of PD-1, PD-L1, perforin, granzyme B, and TRIP13 in tumors of mice treated with vehicle or DCZ0415. E H&E and IHC staining showing infiltration of T cells (CD3 & CD4) and expression PD-1 expression in vehicle- and DCZ0415-treated tumors, Arrows indicate positive staining for CD3, CD4, and PD-1. Scale bar: 20 μm.

combination for tumor weights and tumor volumes. For both tumor weight and in tumor volume reduction, the CI=1, indicating that the effects of combination treatment on tumor weight and tumor volume were additive (Fig. 8B,C). IHC evaluation of tumor tissues revealed that combination treatment further attenuated PCNA, decreased expression of vascular endothelial growth factor (VEGF) and induced active caspase 3 (Fig. 8D). Combination treatment also enhanced the immune response by decreasing expression of PD-1 and facilitating immune cell infiltration of CD3 and CD4 T cells (Fig. 8D). These results demonstrate that the combination treatment effectively reduced PDAC progression by inhibiting proliferation and angiogenesis, inducing apoptosis, enhancing antitumor immunity through infiltration of T cells, and inhibiting the PD1 immune checkpoint.

We assessed whether combining DCZ0415 with gemcitabine enhances anti-metastatic activity in immunocompromised NSG mice. Although DCZ0415 and gemcitabine alone reduced metastasis compared to the vehicle control, the combination treatment demonstrated a substantial reduction in metastasis (Fig. 8E). H&E staining also showed reduced numbers and sizes of metastatic nodules in the lung of mice dosed with the DCZ0415 and gemcitabine combination as compared to DCZ0415 or gemcitabine alone (Fig. 8F). Moreover, the doses of DCZ0415, gemcitabine, or their combination were not toxic to mice (Supplementary Table 6). These results confirm the benefits of combination therapy of TRIP13 inhibition along with gemcitabine in

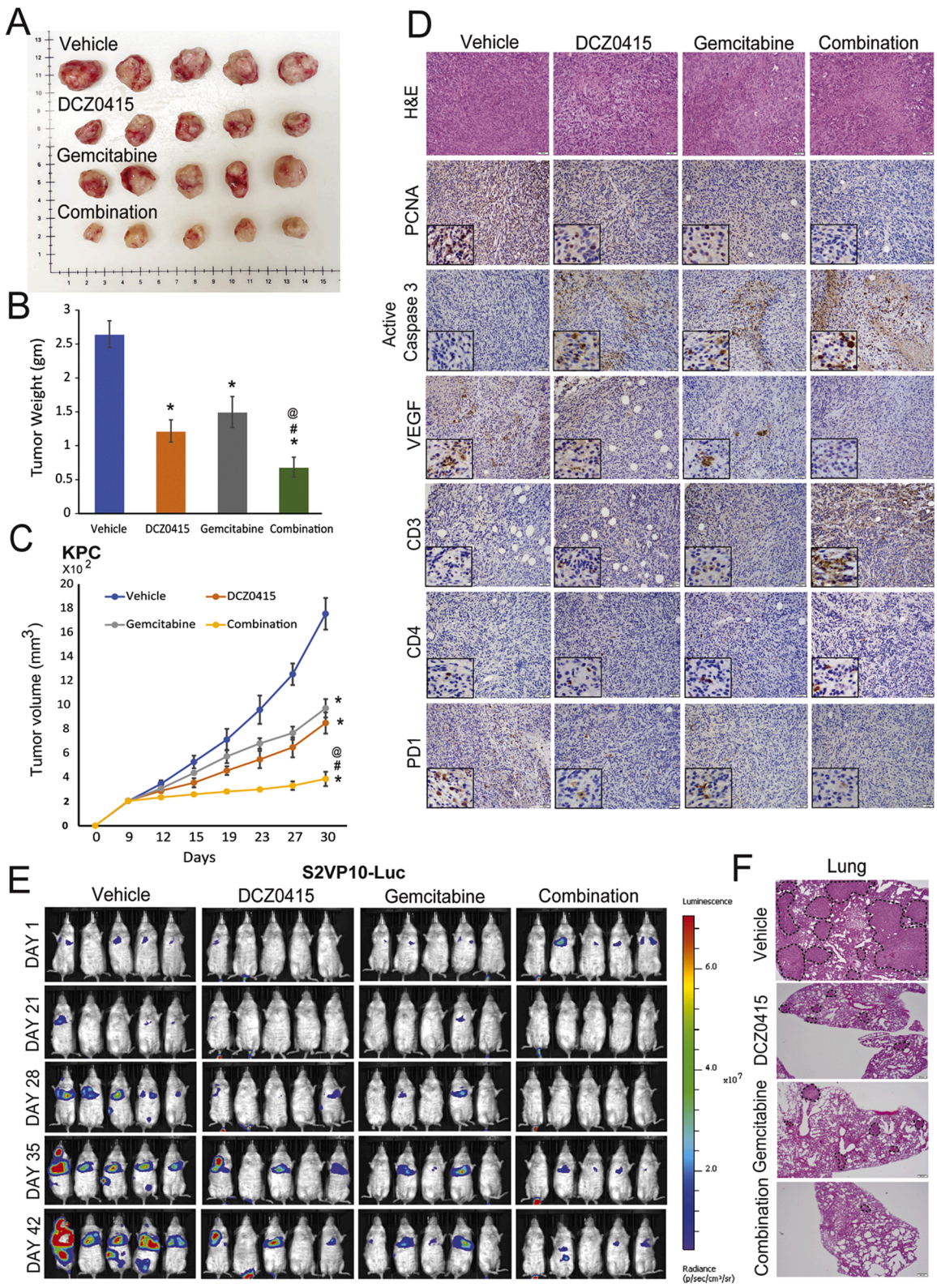

Fig. 8. Impact of DCZ0415, gemcitabine, and their combination on tumor growth, metastasis, and immune response in an immunocompetent syngeneic PDAC mouse model. (A) KPC cells (0.1×10^6) were injected subcutaneously into C57BL/6J mice and treated with vehicle, DCZ0415, gemcitabine, or their combination. Photographs of mouse tumors treated with test agents at termination of the experiment. (B) Tumor weights of mice. Error bars indicate means ± SD, $^{*}P < 0.001$ versus control; $^{\#}P < 0.001$ versus DCZ0415; $^{@}P < 0.001$ versus gemcitabine. (C) Tumor volumes for mice treated with vehicle or DCZ0415. Error bars indicate means ± SD, Error bars indicate means ± SD, $^{*}P < 0.001$ versus control; $^{\#}P < 0.001$ versus DCZ0415; $^{@}P < 0.001$ versus gemcitabine. (D) H&E and immunostaining of T cells (CD3 and CD4) infiltration, immune checkpoint (PD-1), a marker of angiogenesis (VEGF), proliferation (PCNA), and apoptosis (active-caspase-3) were performed for PDAC in tumor-bearing C57BL/6J mice treated as described above. Scale bars: 50 μm. (E) S2VP10- Luc cells (1.0×10^6) were injected into the tail veins of NSG mice. The mice were treated with vehicle, DCZ0415, gemcitabine, or their combination. Metastasis in these mice was monitored every week with an IVIS imaging system. (F) H&E staining showing metastatic lesions in lung (dotted lines). Scale bar: 200 μm.

reducing pancreatic tumor growth and metastasis in pre-clinical models.

Discussion

Pancreatic cancer is the most aggressive cancer with short survival rate from the time of diagnosis. Recent advances in high-throughput technologies enabled identification of driver mutations and oncogenic expression of many targets. However, in pancreatic cancer, there are only few molecular determinants that show genomic aberrations. Thus, there is an urgent need for identification of effective therapeutic targets. We, for the first-time, report the oncogenic role of TRIP13, an AAA-ATPase enzyme, in PDAC and present a strategy to inhibit tumor growth and metastasis by targeting TRIP13. TRIP13 knockdown by shRNA or targeting with the small molecule inhibitor, DCZ0415, reduced malignant phenotypes, tumor growth, and metastasis by down-regulating FGFR4/STAT3/β-catenin and by modulating EMT pathways. Further, DCZ0415 reduced the immunosuppressive tumor microenvironment by increasing cytotoxic mediators (granzyme B and perforin), decreasing immune checkpoints (PD-1 and PD-L1), and facilitating T cell infiltration (CD3 and CD4). Other novel findings are that DCZ0415 in combination with gemcitabine remarkably decreased tumor growth and metastasis by reducing proliferation and angiogenesis, and by enhancing apoptosis and anti-tumor immunity.

In cancers, there is a loss of balance between cell proliferation, cell division, and apoptosis. Apoptosis or "programmed cell death" is an orchestrated biological process for eliminating malignant cells and reducing tumor progression. The mechanisms of cell proliferation and apoptosis are complex and involve Bcl2 family proteins, cell survival markers, and oncogenic signaling pathways [43]. Our studies demonstrated that knockdown of TRIP13 or treatment with DCZ0415 reduced the malignant phenotypes of PDAC cells by decreasing cell proliferation and arresting cells in the G2/M phase of the cell cycle. Knockdown of TRIP13 or treatment of PDAC cells with DCZ0415 also reduced markers of cell proliferation, such as PCNA and cyclin D1. In cancer cells, Bcl-2 family members promote or inhibit cell death by regulating apoptosis [43,44]. TRIP13 knockdown or DCZ0415 treatment of PDAC cells decreased Bcl-2 and increased Bax and Bak proteins, thus favoring apoptosis. This was confirmed by more extensive PARP cleavage in TRIP13-knockdown and DCZ0415-treated PDAC cells. Furthermore, there was reduced tumor growth in TRIP13-knockdown S2VP10 cells. In addition, DCZ0415 treatment decreased tumor growth in immuno-compromised (subcutaneous and orthotropic) and immuno-competent syngeneic mouse models, indicating that TRIP13 is a target of this anti-cancer agent. Our data are in agreement with earlier published work on multiple myeloma [17] and with results of our study in CRC, showing the therapeutic efficacy of DCZ0415 *in vitro* and *in vivo* [28]. The findings show that the oncogenic functions of TRIP13 can be attenuated by targeting with DCZ0415, a small molecule inhibitor, to reduce PDAC progression.

In the present study, we identified mechanisms regulating the oncogenic function of TRIP13 in PDAC growth and progression. Our prior study in CRC demonstrated that TRIP13 interacts with FGFR4 and activates phosphorylation of STAT3 [10]. Moreover, activation of FGFR4 and STAT3 are implicated in PDAC progression [38]. In addition, our observation related to increased expression of TRIP13 in samples with RTK alterations indicate that TRIP13 may be involved in the activation of FGFR4 in PDAC. Thus, the present work focused on evaluating the role of TRIP13 in activation of the FGFR4/STAT3 signaling axis for the first time in PDAC growth, progression, and metastasis. Our results indicate that inhibiting TRIP13 with DCZ0415 inactivates the FGFR4/STAT3 signaling axis, thus establishing TRIP13 as an important therapeutic target in PDAC. The Wnt/β-catenin signaling pathway is involved in the progression and development of drug resistance of various cancers, including PDACs [39,45]. Activated Wnt translocates β-catenin to bind with TCF/LEF transcription factors and to activate a target gene, cyclin D1 [39,46]. Our present results also showed that, in PDAC cells, TRIP13 knockdown as well as DCZ0415 treatment inhibited Wnt/β-catenin signaling, as evidenced by lower levels of active β-catenin; the β-catenin binding factors, TCF1 and LEF1; and a downstream target gene of β-catenin, cyclin D1. These findings show that, in PDAC, knockdown of TRIP13 inactivates the FGFR4/STAT3 axis and the Wnt/β-catenin signaling pathway.

The EMT is defined as a biological process in which cancer cells lose their epithelial characteristics of cell–cell adhesion and gain mesenchymal characteristics of motility and spindle shape for migration and invasion [47]. During the EMT, the expression of E-cadherin, an epithelial marker, is downregulated; whereas the expressions of vimentin and N-cadherin, mesenchymal markers, are upregulated [48]. Our study showed a clear role for TRIP13 in regulating the EMT process and that treatment with DCZ0415 reduces the expression of mesenchymal markers (N-cadherin and vimentin) and increases the expression of an epithelial marker (E-cadherin) in PDAC.

Metastasis is a multistep process in which cancer cells become detached from the primary site of origin and disseminate to distant sites, where they grow and proliferate [49,50]. In PDAC, like in other malignancies, metastasis is associated with a poor prognosis [51]. Prior studies of HCC [8] and CRC [10] show that TRIP13 is linked with metastasis; in the present work, we showed that, with an experimental metastasis model, knockdown of TRIP13 or treatment with DCZ0415 resulted in reducing metastasis of PDAC.

In cancer, PD-L1 is a trans-membrane protein that binds to its receptor PD-1, suppresses T cell infiltration, and promotes tumor escape from the immune system [52,53]. Targeting of PD1/PD-L1 immune checkpoints improves overall survival of patients in various cancers [54]. Thus, we investigated the effect of DCZ0415 treatment on the immune response in an immunocompetent PDAC syngeneic mouse model. Inhibition of TRIP13 by DCZ0415 suppressed PD1/PD-L1 expression and increased T cell infiltration into the tumor microenvironment, thereby promoting antitumor immunity and inhibiting PDAC progression. Activation of STAT3 is involved in regulating PD-L1 expression [55,56]. We found that targeting of TRIP13 with DCZ0415 decreased FGFR4 expression and phosphorylation of STAT3, suggesting that DCZ0415 reduces the expression of PD-L1 by targeting the FGFR4/STAT3 axis. Cytotoxic T cells eliminate cancer cells by releasing a serine protease, granzyme B, through the pore-forming protein, perforin [57]. Our studies focused on elucidating the effect of DCZ0415 on cytotoxic mediators in PDAC found that DCZ0415 increased the expression of granzyme B and perforin, resulting in alleviating an immunosuppressive tumor microenvironment.

To treat PDAC, various combinatorial approaches have been employed, but they showed marginal benefits or failed to improve overall survival [58,59]. However, for human papillomavirus-driven cancers, combined inhibition of Aurora kinase and TRIP13 effectively induces apoptosis [18]. For PDAC patients, gemcitabine, a first-line therapeutic drug, provides only a modest survival advantage [60]. Therefore, new combinatorial approaches are needed to increase the anti-tumor potency of gemcitabine for use against PDAC. Thus, the present study assessed the effect of targeting TRIP13 by DCZ0415 in combination with gemcitabine. DCZ0415 in combination with gemcitabine reduced tumor growth by decreasing proliferation (PCNA) and inducing apoptosis (active-caspase 3). Angiogenesis is a process in which new blood vessels are formed for tumor growth and development. VEGF is an angiogenic factor involved in vascular permeability and inflammation [61,62]. Thus, we found lower VEGF expression in tumors of mice treated with DCZ0415 in combination with gemcitabine as compared to mice treated with either drug alone. Notably, combination treatment enhanced cytotoxic T cell infiltration and reduced PD-1 expression, thus promoting anti-tumor immunity. This preclinical study shows that combining a small molecule inhibitor of TRIP13 with gemcitabine could be an effective novel treatment strategy for PDACs exhibiting high levels of TRIP13 expression.

A limitation of DCZ0415 is that, as demonstrated by us and others,

anti-cancer effects of this agent were noted at modestly high concentrations/doses. Thus, there is a need and scope to employ structure-based approaches to develop new/potent analogs of DCZ0415 that could be used in future clinical trials.

Conclusions

In sum, the present investigation, for the first time, established an oncogenic role of TRIP13, an AAA ATPase enzyme, in PDAC. Our preclinical data demonstrated that silencing of TRIP13 by shRNA and targeting TRIP13 by DCZ0415, a specific inhibitor of TRIP13, reduced cell proliferation, migration, invasion, tumor growth, and metastasis by targeting the TRIP13/FGFR4/STAT3 axis and by downregulating the Wnt/β-catenin and EMT signaling pathways. Furthermore, DCZ0415 treatment induced granzyme B/perforin, inhibited PD/PD-L1, and enhanced T cell infiltration, resulting in destruction of tumors. Finally, we showed that DCZ0415 augmented the therapeutic efficacy of gemcitabine by further reducing tumor progression and that it could provide therapeutic benefits to PDACs expressing high levels of TRIP13. Overall, the findings of this investigation demonstrate that TRIP13 is a potential novel therapeutic target for PDAC.

Ethics statement

All human PDAC tissues used in this research were provided by the Anatomic Pathology Division of UAB after obtaining approval from the UAB Institutional Review Board and Ethics Committee (IRB#090513004). Informed consent was obtained from the patients before their tissues were obtained.

Funding Sources

The work presented in this study was supported, in part, by grant 5U54CA118948 and by institutional funds (Department of Pathology and School of Medicine of UAB) awarded to UM. We also acknowledge the grants (P30CA013148) funded for the Tissue Biorepository and imaging facilities, of the UAB OCCC. We also acknowledge the UAB Metabolism Core, which is supported by the UAB Diabetes Research Center (P30DK079626) and the UAB Center for Clinical and Translational Science (UL1TR003096).

Data availability

Included in the manuscript are data generated in this study; additional data are provided in the supplementary information or available on request.

CRediT authorship contribution statement

Farrukh Afaq: Conceptualization, Data curation, Methodology, Formal analysis, Writing – original draft, Writing – review & editing. **Sumit Agarwal:** Conceptualization, Data curation, Methodology, Formal analysis, Writing – review & editing. **Prachi Bajpai:** Data curation, Methodology, Formal analysis, Writing – review & editing. **Sameer Al Diffalha:** Formal analysis, Visualization, Writing – review & editing. **Hyung-Gyoon Kim:** Formal analysis, Writing – review & editing. **Shajan Peter:** Formal analysis, Writing – review & editing. **Moh'd Khushman:** Formal analysis, Writing – review & editing. **Subhash C Chauhan:** Formal analysis, Writing – review & editing. **Priyabrata Mukherjee:** Formal analysis, Writing – review & editing. **Sooryanarayana Varambally:** Formal analysis, Writing – review & editing. **Upender Manne:** Conceptualization, Methodology, Formal analysis, Funding acquisition, Investigation, Project administration, Resources, Writing – review & editing.

Declaration of Competing Interest

All authors state that there are no potential conflicts of interest.

Acknowledgment

We thank Dr. Donald Hill, in the O'Neal Comprehensive Cancer Center (OCCC), for his editorial assistance. We acknowledge the preclinical imaging shared facility of the OCCC, histology support by the UAB-Tissue Biorepository, and the toxicity assessment study by the UAB Metabolism Core.

Supplementary materials

Supplementary material associated with this article can be found, in the online version, at doi:10.1016/j.neo.2023.100951.

References

[1] R.L. Siegel, K.D. Miller, N.S. Wagle, A. Jemal, Cancer statistics, 2023 *CA Cancer J. Clin.* 73 (2023) 17–48.
[2] L. Rahib, B.D. Smith, R. Aizenberg, A.B. Rosenzweig, J.M. Fleshman, L. M. Matrisian, Projecting cancer incidence and deaths to 2030: the unexpected burden of thyroid, liver, and pancreas cancers in the United States, Cancer Res. 74 (2014) 2913–2921.
[3] J. Long, Y. Zhang, X. Yu, J. Yang, D.G. LeBrun, C. Chen, Q. Yao, M. Li, Overcoming drug resistance in pancreatic cancer, Expert Opin. Ther. Targets 15 (2011) 817–828.
[4] S. Lu, J. Qian, M. Guo, C. Gu, Y. Yang, Insights into a crucial role of TRIP13 in human cancer, Comput. Struct. Biotechnol. J. 17 (2019) 854–861.
[5] K. Wang, B. Sturt-Gillespie, J.C. Hittle, D. Macdonald, G.K. Chan, T.J. Yen, S.T. Liu, Thyroid hormone receptor interacting protein 13 (TRIP13) AAA-ATPase is a novel mitotic checkpoint-silencing protein, J. Biol. Chem. 289 (2014) 23928–23937.
[6] L. Dong, H. Ding, Y. Li, D. Xue, Z. Li, Y. Liu, T. Zhang, J. Zhou, P. Wang, TRIP13 is a predictor for poor prognosis and regulates cell proliferation, migration and invasion in prostate cancer, Int. J. Biol. Macromol. 121 (2019) 200–206.
[7] X.Y. Zhou, X.M. Shu, TRIP13 promotes proliferation and invasion of epithelial ovarian cancer cells through Notch signaling pathway, Eur. Rev. Med. Pharmacol. Sci. 23 (2019) 522–529.
[8] M.X. Zhu, C.Y. Wei, P.F. Zhang, D.M. Gao, J. Chen, Y. Zhao, S.S. Dong, B.B. Liu, Elevated TRIP13 drives the AKT/mTOR pathway to induce the progression of hepatocellular carcinoma via interacting with ACTN4, J. Exp. Clin. Cancer Res. 38 (2019) 409.
[9] N. Sheng, L. Yan, K. Wu, W. You, J. Gong, L. Hu, G. Tan, H. Chen, Z. Wang, TRIP13 promotes tumor growth and is associated with poor prognosis in colorectal cancer, Cell Death. Dis. 9 (2018) 402.
[10] S. Agarwal, M. Behring, H.G. Kim, D.S. Chandrashekar, B. Chakravarthi, N. Gupta, P. Bajpai, A. Elkholy, S. Al Diffalha, P.K. Datta, et al., TRIP13 promotes metastasis of colorectal cancer regardless of p53 and microsatellite instability status, Mol. Oncol. 14 (2020) 3007–3029.
[11] Y. Chen, D. Chen, Y. Qin, C. Qiu, Y. Zhou, M. Dai, L. Li, Q. Sun, Y. Jiang, TRIP13, identified as a hub gene of tumor progression, is the target of microRNA-4693-5p and a potential therapeutic target for colorectal cancer, Cell Death Discov. 8 (2022) 35.
[12] H. Wang, C. Yu, X. Gao, T. Welte, A.M. Muscarella, L. Tian, H. Zhao, Z. Zhao, S. Du, J. Tao, et al., The osteogenic niche promotes early-stage bone colonization of disseminated breast cancer cells, Cancer Cell 27 (2015) 193–210.
[13] J. Lan, J. Huang, X. Tao, Y. Gao, L. Zhang, W. Huang, J. Luo, C. Liu, Y. Deng, L. Liu, X. Liu, Evaluation of the TRIP13 level in breast cancer and insights into potential molecular pathways, J. Cell. Mol. Med. 26 (2022) 2673–2685.
[14] W. Dazhi, Z. Mengxi, C. Fufeng, Y. Meixing, Elevated expression of thyroid hormone receptor-interacting protein 13 drives tumorigenesis and affects clinical outcome, Biomark. Med. 11 (2017) 19–31.
[15] Y. Gao, S. Liu, Q. Guo, S. Zhang, Y. Zhao, H. Wang, T. Li, Y. Gong, Y. Wang, T. Zhang, et al., Increased expression of TRIP13 drives the tumorigenesis of bladder cancer in association with the EGFR signaling pathway, Int. J. Biol. Sci. 15 (2019) 1488–1499.
[16] Y. Tao, G. Yang, H. Yang, D. Song, L. Hu, B. Xie, H. Wang, L. Gao, M. Gao, H. Xu, et al., TRIP13 impairs mitotic checkpoint surveillance and is associated with poor prognosis in multiple myeloma, Oncotarget 8 (2017) 26718–26731.
[17] Y. Wang, J. Huang, B. Li, H. Xue, G. Tricot, L. Hu, Z. Xu, X. Sun, S. Chang, L. Gao, et al., A small-molecule inhibitor targeting TRIP13 suppresses multiple myeloma progression, Cancer Res. 80 (2020) 536–548.
[18] S. Ghosh, T. Mazumdar, W. Xu, R.T. Powell, C. Stephan, L. Shen, P.A. Shah, C. R. Pickering, J.N. Myers, J. Wang, et al., Combined TRIP13 and aurora kinase inhibition induces apoptosis in human papillomavirus-driven cancers, Clin. Cancer Res. 28 (2022) 4479–4493.
[19] R. Banerjee, N. Russo, M. Liu, V. Basrur, E. Bellile, N. Palanisamy, C.S. Scanlon, E. van Tubergen, R.C. Inglehart, T. Metwally, et al., TRIP13 promotes error-prone

nonhomologous end joining and induces chemoresistance in head and neck cancer, Nat. Commun. 5 (2014) 4527.
[20] R. Banerjee, M. Liu, E. Bellile, L.B. Schmitd, M. Goto, M.N.D. Hutchinson, P. Singh, S. Zhang, D.P.V. Damodaran, M.K. Nyati, et al., Phosphorylation of TRIP13 at Y56 induces radiation resistance but sensitizes head and neck cancer to cetuximab, Mol. Ther. (2021).
[21] G. Zhang, Q. Zhu, G. Fu, J. Hou, X. Hu, J. Cao, W. Peng, X. Wang, F. Chen, H. Cui, TRIP13 promotes the cell proliferation, migration and invasion of glioblastoma through the FBXW7/c-MYC axis, Br. J. Cancer (2019).
[22] C. Li, J. Xia, R. Franqui-Machin, F. Chen, Y. He, T.C. Ashby, F. Teng, H. Xu, D. Liu, D. Gai, et al., TRIP13 modulates protein deubiquitination and accelerates tumor development and progression of B cell malignancies, J. Clin. Invest. (2021) 131.
[23] L. Xu, Y. Wang, G. Wang, S. Guo, D. Yu, Q. Feng, K. Hu, G. Chen, B. Li, Z. Xu, et al., Aberrant activation of TRIP13-EZH2 signaling axis promotes stemness and therapy resistance in multiple myeloma, Leukemia (2023).
[24] X. Liu, X. Shen, J. Zhang, TRIP13 exerts a cancer-promoting role in cervical cancer by enhancing Wnt/beta-catenin signaling via ACTN4, Environ. Toxicol. 36 (2021) 1829–1840.
[25] Y. Cao, F. Huang, J. Liu, H. Qi, J. Xiao, MiR-129-5p/TRIP13 affects malignant phenotypes of colorectal cancer cells, Histol. Histopathol. 37 (2022) 879–888.
[26] X. Zhang, J. Zhou, D. Xue, Z. Li, Y. Liu, L. Dong, MiR-515-5p acts as a tumor suppressor via targeting TRIP13 in prostate cancer, Int. J. Biol. Macromol. 129 (2019) 227–232.
[27] B.A. Weir, M.S. Woo, G. Getz, S. Perner, L. Ding, R. Beroukhim, W.M. Lin, M. A. Province, A. Kraja, L.A. Johnson, et al., Characterizing the cancer genome in lung adenocarcinoma, Nature 450 (2007) 893–898.
[28] S. Agarwal, F. Afaq, P. Bajpai, H.G. Kim, A. Elkholy, M. Behring, D. S. Chandrashekar, S.A. Diffalha, M. Khushman, S.P. Sugandha, et al., DCZ0415, a small-molecule inhibitor targeting TRIP13, inhibits EMT and metastasis via inactivation of the FGFR4/STAT3 axis and the Wnt/β-catenin pathway in colorectal cancer, Mol. Oncol. 16 (2022) 1728–1745.
[29] B. Chakravarthi, M.D.C. Rodriguez Pena, S. Agarwal, D.S. Chandrashekar, S. A. Hodigere Balasubramanya, F.J. Jabboure, A. Matoso, T.J. Bivalacqua, K. Rezaei, A. Chaux, et al., A role for De Novo purine metabolic enzyme PAICS in bladder cancer progression, Neoplasia 20 (2018) 894–904.
[30] S. Agarwal, B. Chakravarthi, H.G. Kim, N. Gupta, K. Hale, S.A.H. Balasubramanya, P.G. Oliver, D.G. Thomas, I.A. Eltoum, D.J. Buchsbaum, et al., PAICS, a De Novo purine biosynthetic enzyme, is overexpressed in pancreatic cancer and is involved in its progression, Transl. Oncol. 13 (2020), 100776.
[31] S. Agarwal, B. Chakravarthi, M. Behring, H.G. Kim, D.S. Chandrashekar, N. Gupta, P. Bajpai, A. Elkholy, S.A.H. Balasubramanya, C. Hardy, et al., PAICS, a purine nucleotide metabolic enzyme, is involved in tumor growth and the metastasis of colorectal cancer, Cancers (Basel) (2020) 12.
[32] S. Agarwal, M. Behring, K. Hale, S. Al Diffalha, K. Wang, U. Manne, S. Varambally, MTHFD1L, a folate cycle enzyme, is involved in progression of colorectal cancer, Transl. Oncol. 12 (2019) 1461–1467.
[33] A. Sinha, S. Agarwal, D. Parashar, A. Verma, S. Saini, N. Jagadish, A.S. Ansari, N. K. Lohiya, A. Suri, Down regulation of SPAG9 reduces growth and invasive potential of triple-negative breast cancer cells: possible implications in targeted therapy, J. Exp. Clin. Cancer Res. 32 (2013) 69.
[34] Q. Liu, X. Yin, L.R. Languino, D.C. Altieri, Evaluation of drug combination effect using a bliss independence dose-response surface model, Stat. Biopharm. Res. 10 (2018) 112–122.
[35] D.S. Chandrashekar, B. Bashel, S.A.H. Balasubramanya, C.J. Creighton, I. Ponce-Rodriguez, B. Chakravarthi, S. Varambally, UALCAN: a portal for facilitating tumor subgroup gene expression and survival analyses, Neoplasia 19 (2017) 649–658.
[36] D.S. Chandrashekar, S.K. Karthikeyan, P.K. Korla, H. Patel, A.R. Shovon, M. Athar, G.J. Netto, Z.S. Qin, S. Kumar, U. Manne, et al., UALCAN: an update to the integrated cancer data analysis platform, Neoplasia 25 (2022) 18–27.
[37] Y. Zhang, F. Chen, D.S. Chandrashekar, S. Varambally, C.J. Creighton, Proteogenomic characterization of 2002 human cancers reveals pan-cancer molecular subtypes and associated pathways, Nat. Commun. 13 (2022) 2669.
[38] N. Sasaki, F. Gomi, H. Yoshimura, M. Yamamoto, Y. Matsuda, M. Michishita, H. Hatakeyama, Y. Kawano, M. Toyoda, M. Korc, T. Ishiwata, FGFR4 inhibitor BLU9931 attenuates pancreatic cancer cell proliferation and invasion while inducing senescence: evidence for senolytic therapy potential in pancreatic cancer, Cancers (Basel) (2020) 12.
[39] M. Ram Makena, H. Gatla, D. Verlekar, S. Sukhavasi, K.P. M, C.P. K, Wnt/β-catenin signaling: the culprit in pancreatic carcinogenesis and therapeutic resistance, Int. J. Mol. Sci. (2019) 20.
[40] G.P. Otto, B. Rathkolb, M.A. Oestereicher, C.J. Lengger, C. Moerth, K. Micklich, H. Fuchs, V. Gailus-Durner, E. Wolf, M. Hrabě de Angelis, Clinical chemistry reference intervals for C57BL/6J, C57BL/6N, and C3HeB/FeJ mice (Mus musculus), J. Am. Assoc. Lab. Anim. Sci. 55 (2016) 375–386.
[41] W.F. Loeb, F.W. Quimby, Clinical chemistry of laboratory animals, Taylor & Francis: Philadelphia; London, 1999. Vol.
[42] A.M. Lowy, J. Knight, J. Groden, Restoration of E-cadherin/beta-catenin expression in pancreatic cancer cells inhibits growth by induction of apoptosis, Surgery 132 (2002) 14–148.
[43] B.A. Carneiro, W.S. El-Deiry, Targeting apoptosis in cancer therapy, Nat. Rev. Clin. Oncol. 17 (2020) 395–417.
[44] P.E. Czabotar, A.J. Garcia-Saez, Mechanisms of BCL-2 family proteins in mitochondrial apoptosis, Nat. Rev. Mol. Cell Biol. (2023).
[45] T. Zhan, N. Rindtorff, M. Boutros, Wnt signaling in cancer, Oncogene 36 (2017) 1461–1473.
[46] C. Pilarsky, O. Ammerpohl, B. Sipos, E. Dahl, A. Hartmann, A. Wellmann, T. Braunschweig, M. Löhr, R. Jesenofsky, H. Friess, et al., Activation of Wnt signalling in stroma from pancreatic cancer identified by gene expression profiling, J. Cell. Mol. Med. 12 (2008) 2823–2835.
[47] J.H. Tsai, J. Yang, Epithelial-mesenchymal plasticity in carcinoma metastasis, Genes develop. 27 (2013) 2192–2206.
[48] J.P. Thiery, Epithelial–mesenchymal transitions in tumour progression, Nat. Rev. Cancer 2 (2002) 442–454.
[49] J. Fares, M.Y. Fares, H.H. Khachfe, H.A. Salhab, Y. Fares, Molecular principles of metastasis: a hallmark of cancer revisited, Signal Transduct. Target Ther. 5 (2020) 28.
[50] G.P. Gupta, J. Massagué, Cancer metastasis: building a framework, Cell 127 (2006) 679–695.
[51] T.Y.S. Le Large, M.F. Bijlsma, G. Kazemier, H.W.M. van Laarhoven, E. Giovannetti, C.R. Jimenez, Key biological processes driving metastatic spread of pancreatic cancer as identified by multi-omics studies, Semin. Cancer Biol. 44 (2017) 153–169.
[52] A.H. Sharpe, K.E. Pauken, The diverse functions of the PD1 inhibitory pathway, Nat. Rev. Immunol. 18 (2018) 153–167.
[53] Y. Han, D. Liu, L. Li, PD-1/PD-L1 pathway: current researches in cancer, Am. J. Cancer Res. 10 (2020) 727–742.
[54] Q. Lin, X. Wang, Y. Hu, The opportunities and challenges in immunotherapy: Insights from the regulation of PD-L1 in cancer cells, Cancer Lett. (2023), 216318.
[55] M.J. Kim, H.J. Nam, H.P. Kim, S.W. Han, S.A. Im, T.Y. Kim, D.Y. Oh, Y.J. Bang, OPB-31121, a novel small molecular inhibitor, disrupts the JAK2/STAT3 pathway and exhibits an antitumor activity in gastric cancer cells, Cancer Lett. 335 (2013) 145–152.
[56] Y. Xing, C. Mi, Z. Wang, Z.H. Zhang, M.Y. Li, H.X. Zuo, J.Y. Wang, X. Jin, J. Ma, Fraxinellone has anticancer activity in vivo by inhibiting programmed cell death-ligand 1 expression by reducing hypoxia-inducible factor-1α and STAT3, Pharmacol. Res. 135 (2018) 166–180.
[57] M. Barry, R.C. Bleackley, Cytotoxic T lymphocytes: all roads lead to death, Nat. Rev. Immunol. 2 (2002) 401–409.
[58] F. Lei, X. Xi, S.K. Batra, T.K. Bronich, Combination therapies and drug delivery platforms in combating pancreatic cancer, J. Pharmacol. Exp. Ther. 370 (2019) 682–694.
[59] G. Aprile, F.V. Negri, F. Giuliani, C.E. De, D. Melisi, F. Simionato, N. Silvestris, O. Brunetti, F. Leone, D. Marino, et al., Second-line chemotherapy for advanced pancreatic cancer: which is the best option? Crit. Rev. Oncol. Hematol. 115 (2017) 1–12.
[60] 3rd H.A. Burris, M.J. Moore, J. Andersen, M.R. Green, M.L. Rothenberg, M. R. Modiano, M.C. Cripps, R.K. Portenoy, A.M. Storniolo, P. Tarassoff, et al., Improvements in survival and clinical benefit with gemcitabine as first-line therapy for patients with advanced pancreas cancer: a randomized trial, J. Clin. Oncol. 15 (1997) 2403–2413.
[61] G. Niu, X. Chen, Vascular endothelial growth factor as an anti-angiogenic target for cancer therapy, Curr. Drug Targets 11 (2010) 1000–1017.
[62] P. Carmeliet, Angiogenesis in life, disease and medicine, Nature 438 (2005) 932–936.